Resistive-inductive piezoelectric shunts with negative capacitances and positive position feedback - a comparative study

J. Dietrich [1], **G. Raze** [1], **C. Collette** [2], **A. Deraemaeker** [3], **G. Kerschen** [1]
[1] Space Structures and Systems Laboratory (S3L),
Université de Liège, Quartier Polytech 1 (B52/3), Allée de la Découverte 9, 4000 Liège, Belgium

[2] Active Aerospace Structures and Advanced Mechanical Systems,
Université de Liège, Quartier Polytech 1 (B52/3), Allée de la Découverte 9, 4000 Liège, Belgium

[3] Building Architecture and Town Planning (BATir) Department,
Université Libre de Bruxelles, CP 194/02, av Franklin Roosevelt 50, 1050 Brussels, Belgium

Abstract
By drawing a parallel between the controller parameters of a piezoelectric inductive-resistive (RL) shunt with a negative capacitance (NC) and the active control method positive position feedback (PPF), we prove that there exists an equivalence between the controller parameters and their receptance functions. Based on these findings, exact H_∞ tuning rules for RL shunts are extended to the use of a NC to eventually find optimal values for the design of a PPF controller. In addition, a closed-form expression of the maximum amplitude of the frequency responses is provided. Using these rules, a thorough comparison in terms of performance and stability margins between the RL shunt with NC and the PPF is performed and discussed.

1 Introduction

Based on the piezoelectric effect, self-sensing piezoelectric transducers shunted with an electrical impedance can be used to mitigate the vibrations of engineering structures. The design of this electrical impedance is often realized according to resistive (R) or resistive-inductive (RL) shunt circuit designs [1]. There exist several tuning rules to find optimal values for the resistance and the inductance. On the basis of closed-form solutions for dynamic vibration absorbers introduced by Asami and Nishihara [2], Soltani et al. proposed tuning rules for a RL shunt circuit that lead to minimized equal resonance peaks of the controlled structure [3]. Working according to a passive control law, piezoelectric R or RL shunts are in theory purely passive applications. Their performance depends on the electromechanical coupling between the structure and the piezoelectric transducer. It can be assessed by means of the energy converted by the piezoelectric material, expressed with the so-called effective electromechanical coupling factor (EMCF). For a better authority over the structure, the coupling can be enhanced by using a negative capacitance (NC) in series or in parallel with the shunt circuit. A piezoelectric shunt with a NC includes a NC circuit that needs to be powered while the original shunt circuit works according to a passive control law [4]. However, in current applications, RL shunts can be realized via a digital vibration absorber (DVA), emulating the passive electrical circuit with a digital controller unit [5]. While the control law remains passive, this realization comes with the need for elements of the DVA to be powered.

The idea of a NC has already been introduced in 1979 by Forward when he used a NC in parallel to a piezoelectric transducer for compensation of the inherent capacitance of electromechanical transducers coupled to vibrating mechanical structures [6]. Later, a NC was implemented to cancel the electrical reactance in R shunt circuits, followed by a comparison to RL shunts [7]. A series connection of a NC with a piezoelectric

transducer was exploited Tang and Wang for a better control authority when using RL shunts [8]. Their shunt tuning was based based on common intersection points (fixed points) of resulting frequency response functions (FRFs), introduced by Hagood and von Flotow for passive RL shunts [1]. In 2003, an extensive analytical analysis of piezoelectric R shunts using NCs as well as an experimental demonstration of their findings was conducted by Behrens et al. [9]. Their structure of interest was a plate and the NC values were chosen to be as close as possible to the stability limit [9]. A comparative study of different shunt circuit compositions using R and L elements in series with a NC has been presented by Neubauer et al. to show stability limits and improvements in performance [4]. Their findings have been validated experimentally with a vibrating mass mounted on a piezoelectric stack actuator. Once again, the shunt parameters were set using the fixed-point tuning rules mentioned earlier. Two configurations of a NC, one in series and one in parallel, have been compared by de Marneffe and Preumont with the conclusion that the series implementation was more robust [10]. They validated their findings experimentally on a truss structure with a NC value that was $90\,\%$ of the stability limit. Furthermore, they showed that an integral force feedback (IFF) controller lead to better damping performances than a RL shunt with NC. To account for multiple modes and their influence on the tuning procedure, Berardengo et al. derived more accurate formulations for the dynamic capacitance of a piezoelectric transducer. By using a real circuit for the NC, they designed a robust electrical network that was used in series, in parallel and in a series-parallel combination with RL shunts. Their findings were demonstrated on a cantilever steel beam [11, 12]. Recently, a piezoelectric damping solution targeting multiple modes with R shunts connected to a NC (RNC shunts) was discussed by Berardengo et al.. These RNC shunts were connected to an inductor that was used for enhancement of the broadband attenuation of the RNC shunt to increase its robustness [13].

From an active control perspective, a classic control technique for vibration mitigation is the positive position feedback (PPF) approach where the structure's dynamics are attenuated by a compensator that controls the displacement with an actuation force. It has been inter alia established by Fanson and Caughey [14]. The compensator is acting like a second order filter and the controller is tuned to resonate with the structure's natural frequency. Paknejad et al. proposed a tuning of the PPF controller parameters based on maximum damping using the H_2 norm [15]. They demonstrated their findings on a simple numerical example and experimentally on a cantilever beam. In addition, the influence of the proposed tuning rules on the static response of the controlled system was studied. Zhao et al. already discussed a PPF controller design based on H_∞ tuning using the fixed-point method [16]. As discussed above, this method does not yield exact optimal solutions. Traditionally, when using a PPF controller, the position coordinate measured by a sensor is positively fed to the compensator and positively fed back to the structure via an actuator [14, 17]. From this point of view, this method can thus be seen in contrast to the self-sensing control approach of a shunt. Agnes already pointed out similarities between a NC shunt and a PPF controller in [17]. However, to this date, a complete equivalence between the PPF and a shunt with an NC has not been demonstrated.

In this work, we present a comparison of the two control techniques. First, similarities between classic RL shunts with NC and a PPF controller are pointed out by looking at the dimensionless forms of their receptance functions. Based on these similarities, common tuning rules for RL shunts using H_∞ optimization and aiming for an equal-peak design are extended to, in a first step, find theoretically optimal values for RL shunts with NC. By using the derived parameter equivalence between the the former and the PPF controller, we can then provide exact tuning rules for the PPF controller and a closed-form expression of the maximum amplitude of the frequency responses for both approaches. In addition, a comparison between the RL shunt with NC and the PPF is presented and discussed in terms of performance, open-loop transfer functions and stability margins.

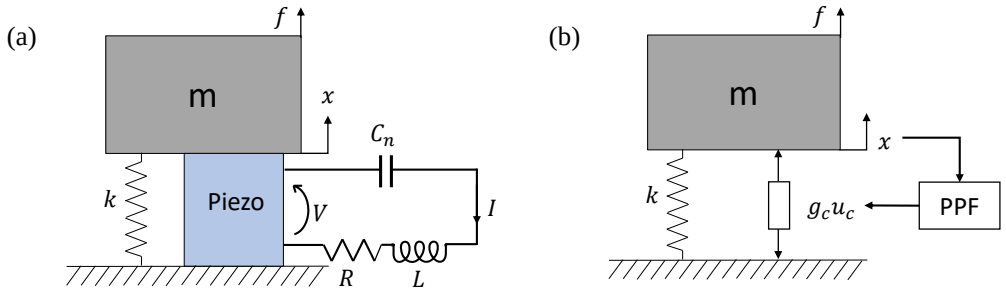

Figure 1: SDOF system with a (a) series RL shunt in series with a NC and (b) PPF controller.

2 Equivalence between a RL shunt with NC and a collocated PPF

2.1 The host system

For a piezoelectric single-degree-of-freedom (SDOF) structure (cf. Figure 1(a)), the equations of motion using the Laplace variable s are given by

$$\begin{cases} mxs^2 + k_{oc}x - \theta q = f \\ \theta x - \frac{1}{C_p^\varepsilon} q = V \end{cases} . \tag{1}$$

x is the displacement, f an external disturbance force, q the electric charge of the electrodes of the piezoelectric transducer and V the voltage across them. m is the mass of the mechanical system, k_{oc} its stiffness when the transducer is in open-circuit and C_p^ε the capacitance of the piezoelectric transducer under constant strain. The equations are related to each other via the electromechanical coupling coefficient θ. This coefficient characterizes how much energy is transformed between the piezoelectric transducer and the mechanical system [1] so that an interaction between the electrical and mechanical dynamics takes place. One can see this when regarding the resonance frequencies of the SDOF oscillator in open-circuit ($q = 0$) and in short-circuit ($V = 0$). In open-circuit, its resonance frequency is $\omega_{oc} = \sqrt{k_{oc}/m}$ while, when in short-circuit, the stiffness of the structure changes according to Equation (1) to

$$k_{sc} = k_{oc} - \theta^2 C_p^\varepsilon. \tag{2}$$

In this way, the resonance frequency becomes $\omega_{sc} = \sqrt{k_{sc}/m}$.

2.2 The RL shunt with NC

When piezoelectric shunts are used for vibration mitigation, the authority over the system depends on the electromechanical coupling. A way to assess this coupling is the dimensionless EMCF K_c that relates the modal strain energy when the transducer is in short- and in open-circuit to each other [18]:

$$K_c^2 = \frac{\omega_{oc}^2 - \omega_{sc}^2}{\omega_{sc}^2} . \tag{3}$$

Thus, this coupling factor depends on the fixed properties of the host system represented by the parameters θ and C_p^ε in Equation (2). In Equation (3), the short-circuit resonance frequency is used for normalization. One could likewise normalize with ω_{oc}, defining the EMCF as

$$\alpha^2 = \frac{\omega_{oc}^2 - \omega_{sc}^2}{\omega_{oc}^2} = \frac{K_c^2}{1 + K_c^2} . \tag{4}$$

In piezoelectric shunt damping, a RL shunt connected to the electrodes of the transducer needs to be properly tuned to mitigate the resonance amplitude of the structural response. Here, the EMCF determines the maximum amplitude of the forced response of the controlled system [3]. Adding a NC to the shunt circuit can enhance the EMCF by increasing the coupling [10]. While a NC can be added to any passive shunt, it is usually realized with an active component, such as an operational amplifier. Thus, instabilities can occur if the NC is not properly selected.

When the piezoelectric transducer is connected to a classic RL shunt circuit in series with a negative capacitance C_n, we obtain the following relation between the voltage and the charge

$$\left(Ls^2 + Rs - \frac{1}{C_n}\right) q = V. \tag{5}$$

Thus, the electrical part of Equation (1) reads

$$Ls^2 q + Rsq + \frac{1}{C_{eff}} q - \theta x = 0. \tag{6}$$

We introduce the effective capacitance [11]

$$\frac{1}{C_{eff}} = \frac{1}{C_p^\varepsilon} - \frac{1}{C_n}. \tag{7}$$

To achieve an optimal damping performance, the shunt parameters R and L need to be tuned in dependence of the chosen C_n. In a first step, the transfer function from the disturbance force to the displacement is regarded. From Equations (1) and (6), we obtain

$$\frac{x}{f} = \left[ms^2 + k_{oc} - \frac{\theta^2}{Ls^2 + Rs + \frac{1}{C_{eff}}}\right]^{-1}. \tag{8}$$

Equation (8) can be written in dimensionless form using the electrical frequency and the damping ratio of the shunt

$$\omega_e^2 := \frac{1}{C_{eff} L}, \;\; 2\omega_e \zeta_e := \frac{R}{L} \tag{9}$$

and [19]

$$x_{st} := \frac{f}{k_{oc}}, \;\; \tilde{\alpha}^2 := \frac{\theta^2 C_{eff}}{k_{oc}}, \;\; \nu_e := \frac{\omega_e}{\omega_{oc}}, \;\; \hat{s} := \frac{s}{\omega_{oc}}. \tag{10}$$

Using Equations (9) and (10), the transfer function of the SDOF system with the piezoelectric shunt in dimensionless form is

$$h(\hat{s}) = \frac{x}{x_{st}} = \left[\hat{s}^2 + 1 - \frac{\tilde{\alpha}^2}{\frac{\hat{s}^2}{\nu_e^2} + 2\zeta_e \frac{\hat{s}}{\nu_e} + 1}\right]^{-1}, \tag{11}$$

with tilde referring to the case when negative capacitance is used. With Equations (4), (7) and (10), the enhanced EMCF is now

$$\tilde{\alpha}^2 = \frac{\theta^2 C_p^\varepsilon}{k_{oc}} \frac{C_{eff}}{C_p^\varepsilon} = \alpha^2 \left[1 - \frac{C_p^\varepsilon}{C_n}\right]^{-1}. \tag{12}$$

It is is greater than the base EMCF when $C_p^\varepsilon < C_n < \infty$. Given that

$$\tilde{K}_c^2 = \frac{\tilde{\alpha}^2}{1 - \tilde{\alpha}^2}, \tag{13}$$

the short-circuit normalized EMCF is also increased.

Table 1: Equivalence between the dimensionless parameters of a NC shunt and a PPF controller.

Shunt	$\tilde{\alpha}^2$	ν_e	ζ_e
PPF	g	ν_c	ζ_c

2.3 The PPF controller

The active control approach using a PPF controller (cf. Figure 1(b)) is now taken into account, considering a collocated sensor and actuator. The equations of motion read

$$\begin{cases} mxs^2 + kx = f + \omega_c^2 g_c u_c \\ (s^2 + 2\omega_c\zeta_c s + \omega_c^2)u_c = x \end{cases} . \tag{14}$$

The variables u_c, ζ_c, ω_c and g_c refer to the control signal, damping ratio, frequency and gain of the controller, respectively. Inserting the second line of Equation (14) in the first yields

$$(ms^2 + k)x = f + \frac{\omega_c^2 g_c x}{s^2 + 2\omega_c\zeta_c + \omega_c^2}. \tag{15}$$

Dividing Equation (15) by x and forming its reciprocal results in the receptance function

$$\frac{x}{f} = \left[ms^2 + k - \frac{\omega_c^2 g_c}{s^2 + 2\omega_c\zeta_c s + \omega_c^2}\right]^{-1}. \tag{16}$$

Using [19]

$$x_{st} := \frac{f}{k},\ \omega_0 := \sqrt{\frac{k}{m}},\ \hat{s} := \frac{s}{\omega_0},\ \nu_c := \frac{\omega_c}{\omega_0},\ g := \frac{g_c}{k}, \tag{17}$$

we can now write Equation (16) in dimensionless form:

$$\frac{x}{x_{st}} = \left[\hat{s}^2 + 1 - \frac{g}{\frac{\hat{s}^2}{\nu_c^2} + 2\zeta_c\frac{\hat{s}}{\nu_c} + 1}\right]^{-1} . \tag{18}$$

2.4 Equivalence between the RL shunt with NC and a self-sensing PPF

From Equations Equations (11) and (18), we note a parameter equivalence reported in Table 1. Agnes already noted a dynamical similarity between the RL shunt and PPF in [17]. In this study, we further highlight a *full equivalence* between the two approaches in terms of tuning parameters (cf. Table 1) and their receptance functions.

From the previous developments, it can be stated that in this context the NC shunt corresponds to a self-sensing PPF controller: The piezoelectric transducer is actuated by its charge and the position is estimated by its voltage. In fact, the electrical part of Equation (1) reads

$$x = \frac{1}{\theta}\left(V + \frac{1}{C_p^\varepsilon}q\right), \tag{19}$$

and, considering the mechanical part of Equation 1, the force defined by the PPF controller acts on the structure if the following relation holds true:

$$\omega_c^2 g_c u_c = \theta q. \tag{20}$$

A combination of the transfer function of the PPF given in the second line of Equation (14) with Equations

(14) and (20) yields the relation between the charge and voltage applied by the self-sensing PPF

$$\left[\frac{\theta^2}{\omega_c^2 g_c}\left(s^2+2\zeta_c\omega_c s+\omega_c^2\right)-\frac{1}{C_p^{\varepsilon}}\right]q=V. \tag{21}$$

With the parameters given in Equations (10) and (17) (with $k=k_{oc}$),

$$\frac{\theta^2}{g_c}=\frac{\theta^2}{k\alpha^2}=\frac{1}{C_{eff}}. \tag{22}$$

Using the definition of the effective capacitance (Equation (7)) and the parameter equivalence in Table 1, Equation (21) is indeed identical to Equation (5). Thus, an equality between a self-sensing PPF and a RL shunt with series NC is proven.

3 H_∞ tuning rules

Exact tuning rules for passive RL shunts have already been introduced by Soltani et al. in [3]. They minimized the H_∞ norm of the receptance function to obtain two resonance peaks of equal amplitude. Thanks to the incorporation of a NC, a free parameter $\tilde{\alpha}$ is now added in the shunt approach. First, we fix the parameter $\tilde{\alpha}$ to find optimal values for ν_e and ζ_e by minimizing the H_∞ norm of the transfer function $h(i\hat{\omega})$. Here, i is the unit imaginary number and $\hat{\omega}$ a circular frequency normalized by ω_{oc} given in Equation (11):

$$\min_{\nu_e,\zeta_e}\|h(i\hat{\omega}_e)\|_\infty \rightarrow \text{find } \nu_e,\zeta_e \text{ such that } \; |h(i\hat{\omega}_{e,A})|=|h(i\hat{\omega}_{e,B})|\equiv h_0.$$

h_0 is the maximum amplification of two equal resonance peaks that are located at dimensionless frequencies $\hat{\omega}_{e,A}$ and $\hat{\omega}_{e,B}$. We can express h_0 as a function of $\tilde{\alpha}$ [3]:

$$h_0=\frac{8}{\tilde{\alpha}\sqrt{2\sqrt{54\tilde{\alpha}^4-144\tilde{\alpha}^2+64}+9\tilde{\alpha}^2+16}} \tag{23}$$

and solve the equation to $\tilde{\alpha}$. Equation (23) can be shown to be equivalent to

$$135h_0^4\tilde{\alpha}^8-864h_0^4\tilde{\alpha}^6+1152h_0^2\tilde{\alpha}^4+2048h_0^2\tilde{\alpha}^2-4096=0. \tag{24}$$

This quartic equation in $\tilde{\alpha}^2$ is theoretically solvable in closed-form so that, from a desired amplification h_0, we can find a respective coupling coefficient $\tilde{\alpha}^2$ by solving Equation (24).

The peak amplitude h_0 is now to be minimized and a value for $\tilde{\alpha}$ shall be found where

$$\frac{\partial h_0}{\partial\tilde{\alpha}}=0\,. \tag{25}$$

The following expression is found [20]:

$$\frac{\partial h_0}{\partial\tilde{\alpha}}=-\frac{4\left(\frac{216\tilde{\alpha}^3-288\tilde{\alpha}}{\sqrt{54\tilde{\alpha}^4-144\tilde{\alpha}^2+64}}+18\tilde{\alpha}\right)}{\tilde{\alpha}\left(9\tilde{\alpha}^2+2\sqrt{54\tilde{\alpha}^4-144\tilde{\alpha}^2+64}+16\right)^{3/2}}-\frac{8}{\tilde{\alpha}^2\sqrt{9\tilde{\alpha}^2+2\sqrt{54\tilde{\alpha}^4-144\tilde{\alpha}^2+64}+16}}\,. \tag{26}$$

Solving Equations (23) and (25) for $\tilde{\alpha}$ yields

$$\tilde{\alpha}_{opt}=2\sqrt{\frac{2}{15}}\,. \tag{27}$$

The minimum attainable H_∞ norm can be found by inserting $\tilde{\alpha}_{opt}$ in Equation (23):

$$h_{0,opt}=\sqrt{5}. \tag{28}$$

Using $\tilde{\alpha}_{opt}$, the tuning parameters ν_e and ζ_e shall now be found. They can be expressed as a function of $\tilde{K}_c^2$ (cf. Equation (13)) using the tuning rules provided by Soltani et al. [3]. With the intermediate parameter

$$r = \frac{\sqrt{64 - 16\tilde{K}_c^2 - 26\tilde{K}_c^4} - \tilde{K}_c^2}{8}, \tag{29}$$

the optimal frequency and damping ratios are

$$\nu_e = \sqrt{\frac{3\tilde{K}_c^2 - 4r + 8}{4\tilde{K}_c^2 + 4}} \tag{30}$$

and

$$\zeta_e = \frac{\sqrt{27\tilde{K}_c^4 + 80\tilde{K}_c^2 + 64 - 16r\left(4 + 3\tilde{K}_c^2\right)}}{\sqrt{2}\left(5\tilde{K}_c^2 + 8\right)}, \tag{31}$$

respectively.

For the RL shunt with NC, we can find a theoretical optimal value for C_n from Equations (12) and (27)

$$C_{n,opt} = C_p^{\varepsilon}\left[1 - \frac{\alpha^2}{\tilde{\alpha}_{opt}^2}\right]^{-1}. \tag{32}$$

With Equation (9), the shunt parameters R and L can be derived for a series shunt by expressing them in terms of C_{eff}, ω_{oc}, ν_e and ζ_e. Likewise, we can define optimal values for the PPF controller by using $\tilde{\alpha}_{opt}^2$ from Equation (27) together with Equations (30) and (31) in combination with the relations given in Table 1.

3.1 Discussion of the derived tuning rules

The parameter equivalence that was shown in the current section enabled the use of common tuning rules for the shunt and the PPF controller. These two control approaches can theoretically attain the same performance when $\tilde{\alpha}^2$ and g are equal, and Equation (28) features a lower bound for the H_∞ norm attainable by both approaches. This bound is reached when $\tilde{\alpha}$ assumes its optimal value given by Equation (27). Hence, this may lead us to conclude that both approaches are fully equivalent. However, practical considerations discussed in the next section will show that the PPF is the only viable alternative when one desires to attain this optimal performance. These optimal tuning rules are thus particularly useful for the PPF controller. In contrast, the NC should rather be considered as a parameter that improves the authority over the structure and that does not need to be explicitly optimized. With the practical consideration of ensuring sufficient stability margins, one should therefore pick a value of C_n resulting from a trade-off between robustness margins and performance, rather than computing it from Equation (32). The corresponding value of $\tilde{\alpha}$ can then be deduced from Equation (12).

4 Performance and comparison

In the following, the derived tuning rules are used for the NC shunt and the PPF controller to adopt the same controller parameters for both approaches. They are compared in terms of performance, open-loop transfer functions and stability.

4.1 Performance

The performance of the NC shunt and the PPF controller shall now be compared to each other by means of a numerical example. To this end, a dimensionless SDOF system is exploited and the transfer functions between the structural response and the external disturbance force (Equations (11) and (18)) are compared in Figure 2. Both approaches, properly tuned, lead to a successful attenuation of the resonance amplitude.

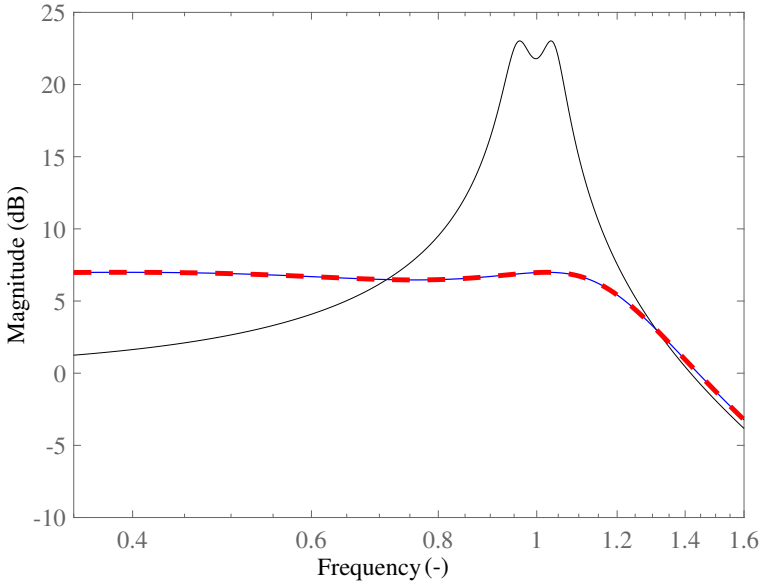

Figure 2: FRFs between structural response and external disturbance force of a SDOF system controlled by a piezoelectric series RL shunt circuit with a NC (—) and a PPF controller (—) in contrast to a fully passive RL shunt ($\alpha = 0.1$) (—).

In addition, it can be seen that their damping performance is indeed identical. The frequency response function (FRF) of the receptance with a passive RL shunt is plotted for comparison. Here, α was chosen to 0.1. Figure 2 highlights that the NC shunt and the PPF approach lead to a clearly better reduction of the resonance amplitude. However, there is a trade-off between this amplitude reduction and the static response. We observe that, in the case of the NC shunt or the PPF controller, the static response grows and that the system is softening. Interestingly, Paknedjad et al. made the same observations in their work. They designed a PPF controller based on maximum damping using a H_2 optimization of the receptance [15]. Considering the here proposed H_∞ tuning rules, there is a relation between the parameter $\tilde{\alpha}$ and the system's stiffness. Indeed, the evaluation of Equation (11) at $\hat{s} = 0$ gives the static response

$$h(0) = \frac{1}{1 - \tilde{\alpha}^2}, \tag{33}$$

which grows with $\tilde{\alpha}$. Different FRFs for variations of this parameter based on its optimal value in the H_∞ sense are displayed in Figure 3, using the example of a NC shunt. If $\tilde{\alpha} < \tilde{\alpha}_{opt}$, the static response is smaller than in the optimal case but the magnitude of the resonance amplitude is greater so that $h_0 > h_{0,opt}$ (cf. Figure 3). Soltani et al. stated that α should not be chosen higher than $\tilde{\alpha}_{max} = 0.74815$ [3]. Figure 4 shows the maximum amplitude of the receptance function h_0 as well as the amplitude of the static response in dependence of the value $\tilde{\alpha}$. Indeed, for values of $\tilde{\alpha}$ chosen to be greater than this $\tilde{\alpha}_{max}$, the equal-peak design of the receptance function becomes ineffectual and the maximum of the receptance function is shifted to $\hat{s} = 0$. It can thus be stated that the minimum amplitude given in Equation (28) is the only minimum and that the value found for $\tilde{\alpha}_{opt}$ is indeed an unique optimum. In contrast to the fixed-point method, the here proposed closed-form solution of the resonance amplitude and its H_∞ optimization allows to take the system's stiffness into account and to limit the static softening.

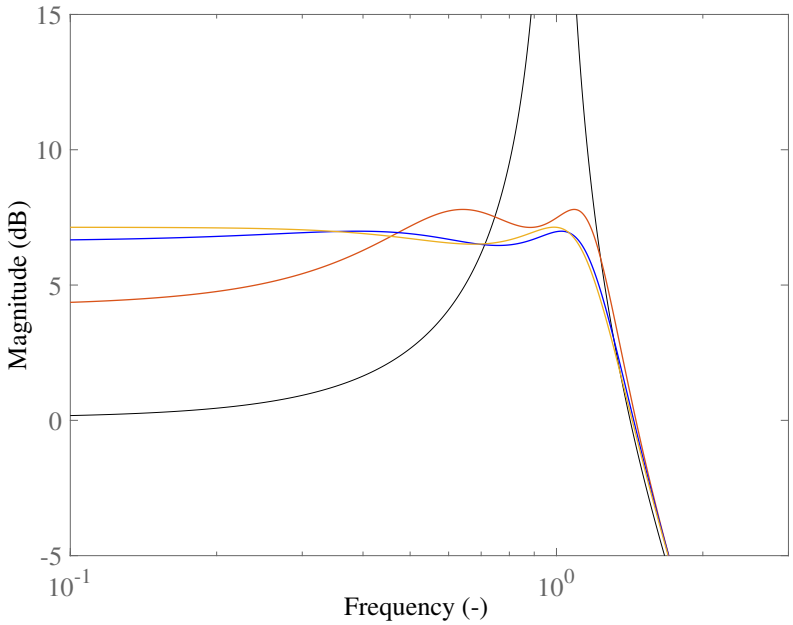

Figure 3: FRFs between structural response and external disturbance force of a SDOF system controlled by a piezoelectric series RL shunt circuit with a NC in contrast to a fully passive RL shunt (—). The parameter for the NC has been chosen according to $\tilde{\alpha} = 0.85\tilde{\alpha}_{opt}$ (—), $\tilde{\alpha} = \tilde{\alpha}_{opt}$ (—) and $\tilde{\alpha} = 1.025\tilde{\alpha}_{opt}$ (—).

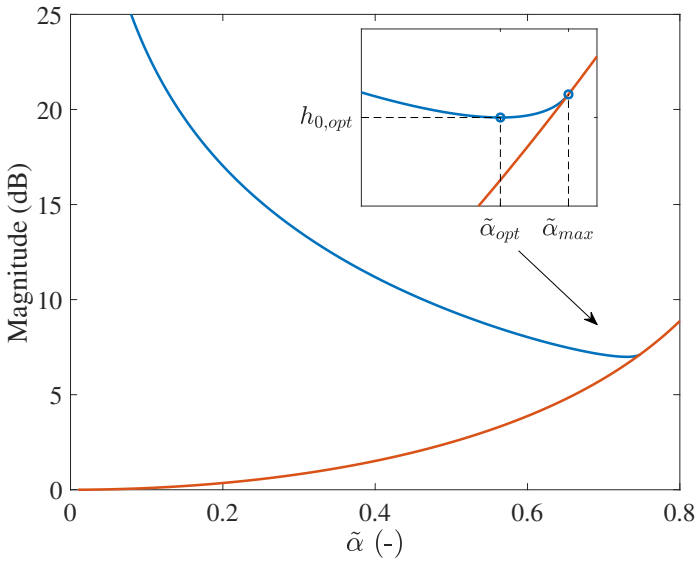

Figure 4: Maximum amplitude h_0 (—) and static response (—) of the SDOF system with a NC shunt in dependence of $\tilde{\alpha}$.

4.2 Open-loop transfer functions

In the following, the open-loop transfer functions of the SDOF system with a NC shunt and a PPF controller are derived from the schematics displayed in Figure 5. For the piezoelectric shunt, the open-loop transfer functions are built by means of the voltage measured by the piezoelectric transducer and the current defined by the controller function. Thus, the plant transfer function $G_{Shunt}(s)$ is defined as the transfer function between sq and V when the external forcing f is set to zero. This function is also known as the dynamic

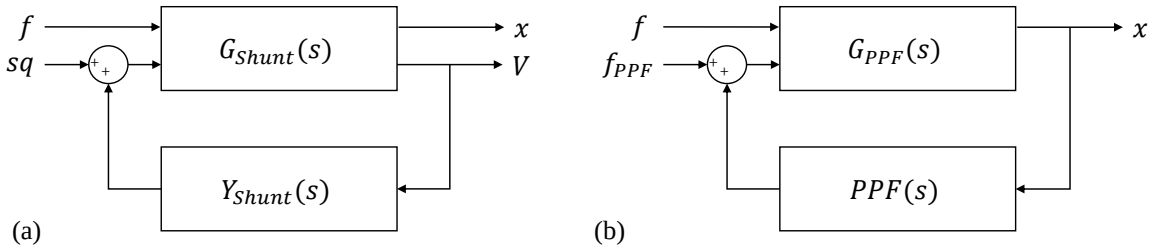

Figure 5: Feedback control with a piezoelectric RL shunt with NC (a) and with PPF (b).

impedance of the piezoelectric transducer. In practice, this relation is usually measured and used for the shunt tuning. From Equations (1) and (2),

$$G_{Shunt}(s) = \left.\frac{V}{sq}\right|_{f=0} = -\frac{1}{sC_p^{\varepsilon}}\frac{s^2+\omega_{sc}^2}{s^2+\omega_{oc}^2}. \tag{34}$$

Here, the shunt admittance

$$Y_{Shunt} = \frac{1}{Ls + R - \frac{1}{sC_n}} \tag{35}$$

is seen as the feedback controller, having V as its input and sq as the output. We now combine Equations (34) and (35) to obtain the open-loop transfer function in dimensionless form (with Equations (9) and (10)):

$$H_{ol,Shunt}(\hat{s}) = -G_{Shunt}(\hat{s})Y_{Shunt}(\hat{s}) = \frac{\hat{s}^2+1-\alpha^2}{\hat{s}^2+1}\frac{\frac{\tilde{\alpha}^2}{\alpha^2}}{\frac{\hat{s}^2}{\nu_e^2}+2\zeta_e\frac{\hat{s}}{\nu_e}+1-\frac{\tilde{\alpha}^2}{\alpha^2}}. \tag{36}$$

The open-loop transfer function of the system with the PPF controller includes the plant transfer function $G_{PPF}(s)$ that can be derived from Equation (14). It is the transfer function between the controller force $f_{PPF} = \omega_c^2 g_c u_c$ and the displacement x when $f = 0$:

$$G_{PPF}(s) = \frac{1}{ms^2+k}. \tag{37}$$

The PPF controller function is the second-order filter

$$PPF(s) = \frac{g_c\omega_c^2}{s^2+2\omega_c\zeta_c s+\omega_c^2}. \tag{38}$$

Using Equations (37) and (38), and the parameters in Equation (17), the open-loop transfer function in dimensionless form is

$$H_{ol,PPF}(\hat{s}) = -G_{PPF}(\hat{s})PPF(\hat{s}) = -\frac{1}{\hat{s}^2+1}\frac{g}{\frac{\hat{s}^2}{\nu_c^2}+2\zeta_c\frac{\hat{s}}{\nu_c}+1}. \tag{39}$$

4.3 Stability

In order to explain the stability of the controlled systems, we consider the expressions of the open-loop transfer functions given in Equations (36) and (39). Previous works have shown that as long as the damping ratio and optimal frequency are greater than zero, the only parameter that could de-stabilize the controller could be $\tilde{\alpha}$, or g respectively [10, 21]. It can thus be seen as the decisive parameter for stability. For the system with a RL shunt with NC, we also have to consider the initial electromechanical coupling, given by α. With strong initial coupling, we have better authority of the passive system and the system is more

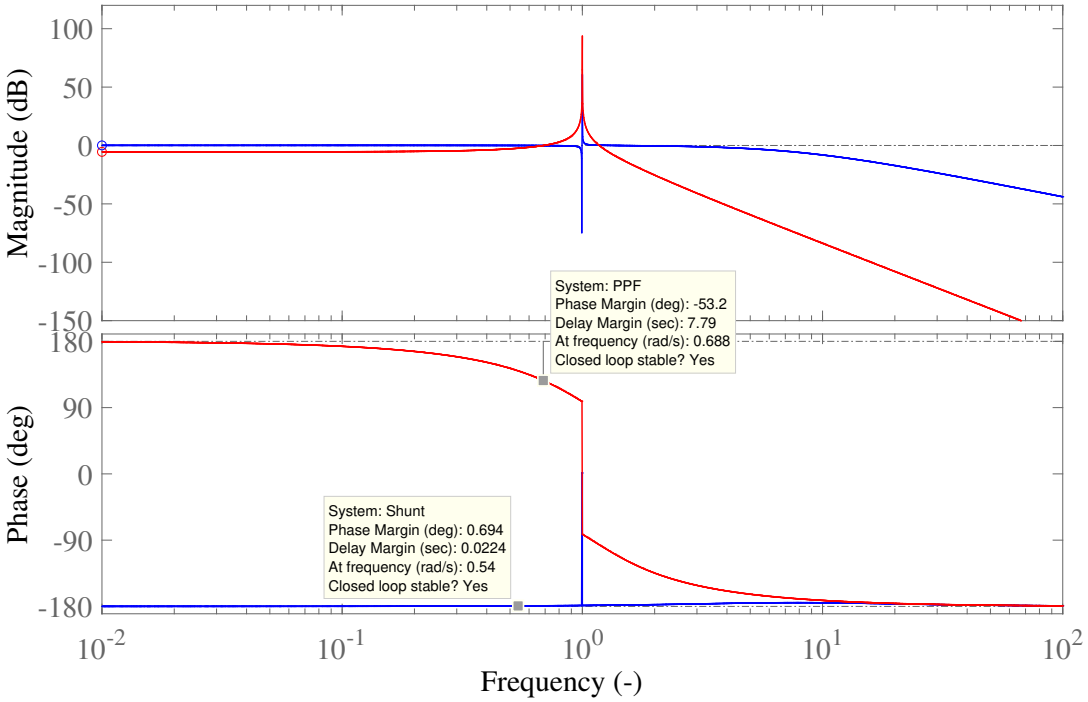

Figure 6: Bode plots of the open-loop transfer functions of a dimensionless SDOF system with a RL shunt with NC (—) and a PPF controller (—) tuned according to H_∞ tuning rules.

robust. Taking into account that a RL shunt with a NC already has small stability margins, we further note that the here proposed $C_{n,opt}$ (cf. Equation (32)) is already close to a theoretical stability limit defined by de Marneffe and Preumont [10]. They state that the controlled system with a piezoelectric series shunt circuit in series with a NC is stable if

$$C_n > \frac{\omega_{oc}^2}{\omega_{sc}^2} C_p^\varepsilon. \tag{40}$$

A stability limit is reached when the structure's stiffness (as it is seen from the transducer) is cancelled out by the negative stiffness of the transducer, represented by the capacitance ($\omega_{oc}^2 C_p^\varepsilon / \omega_{sc}^2 = C_n$) [10]. A look at Equation (12) reveals that, in this case, $\tilde{\alpha}^2 = 1$, thus stability is ensured if $\tilde{\alpha}^2 < 1$. This is in line with the stability limit for the gain of a PPF controller $g < 1$, given by Zhao et al. [21].

4.4 Stability margins

Closed-loop stability is a necessary requirement to guarantee the performance a control system but it is not a sufficient one. In practice, one has to ensure sufficient stability margins to account for uncertainties and unmodeled dynamics in the system. These margins can be deduced from the open-loop transfer functions [22]. When comparing the open-loop transfer functions given in Equations (36) and (39), one can see that they are not identical. This can be explained by the different implementations of the controllers. In the shunt approach, only the function $Y_{Shunt}(s)$ is regarded as the feedback, acting on a plant that includes the piezoelectric coupling - a point of view that is motivated by the actual practical implementation of piezoelectric shunts. Considering the PPF, the plant consist only of the mechanical system.

Figure 6 displays the Bode plots of the derived open-loop transfer functions for the SDOF system (cf. Equations (36) and (39)) in the optimal tuned case (cf. Section 3). It can be seen that the transfer functions of $H_{ol,Shunt}(\hat{s})$ and $H_{ol,PPF}(\hat{s})$ evolve in a different way and that the PPF controller provides considerably

greater stability margins in the region of the resonance. We can thus expect differences in the robustness margins of the two approaches.

Figure 7 displays the phase margins for both approaches in dependence on the choice of the parameter $\tilde{\alpha}$. Considering the NC shunt, the phase margins decrease drastically for values of $\tilde{\alpha}$ that are roughly larger than 0.1. For values close to $\tilde{\alpha}_{opt}$, there is nearly no phase margin left. These extremely small phase margins featured by the NC shunt make its implementation difficult if not impossible. In particular, with a phase margin of less than $1°$, the optimal NC shunt is not implementable in practice. Indeed, this would make the application extremely sensitive to delays induced by e.g. digital controllers [23]. To obtain a decent phase margin, one has to choose a smaller coupling coefficient $\tilde{\alpha}$ than the optimal one (cf. Figure 7). In contrast to the NC shunt, the phase margins obtained with a PPF controller are considerably larger which makes this approach robust and viable in practical applications.

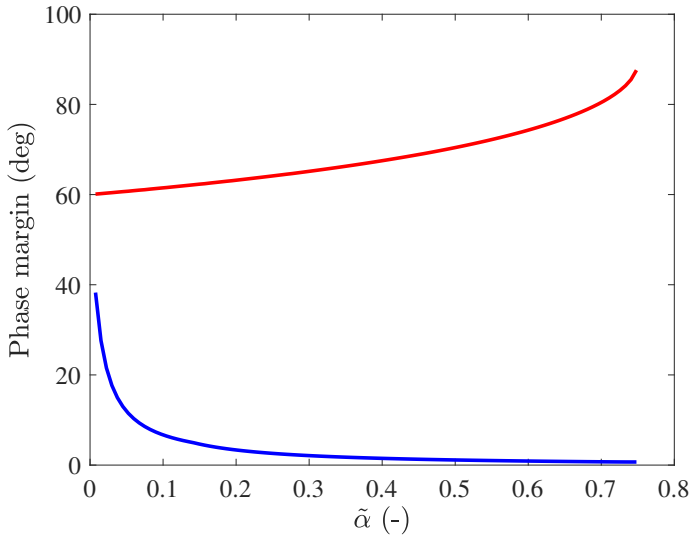

Figure 7: Phase margins for the open-loop transfer functions of the RL shunt with NC (—) and the PPF controller (—) for variations of the parameter $\tilde{\alpha}$.

4.5 Implementation

Finally, we regard the practical implementation of the here discussed control approaches. While a RL shunt with a NC necessarily requires the usage of a piezoelectric transducer, a PPF controller can be realized with any pair of sensor/actuator and can thus be seen as a more general approach. Another advantage of the PPF controller is that less knowledge about the system plant is necessary to design the controller. Using the PPF, only the parameters k and ω_0 need to be known to define the controller function. In contrast, due to the fact that the electromechanical system is regarded as the plant function in piezoelectric shunt damping, three system parameters need to be known for the tuning of the NC shunt: ω_{sc}, ω_{oc} and C_p^{ε}. Keeping in mind that a correct identification of the system parameters can often be challenging, it can be advantageous that fewer parameters are required for the design of the PPF controller. However, for the theoretical developments in this work, a collocated control is assumed for the realization of the PPF controller. It needs to be taken into account that the realization might not always be feasible and how a non-perfectly collocated setup will impact the damping performance.

5 Conclusions and outlook

By proving that the receptance functions of a RL shunt with NC and a collocated PPF controller are equivalent, we derived new optimal tuning rules in the H_∞ sense for the PPF controller aiming for an equal-peak design. In addition, we provided an expression of the resonance amplitude in closed-form. The here proposed tuning rules prove to yield a strong reduction of the resonance amplitude demonstrated on a SDOF system. It has to be mentioned that this amplitude reduction comes at the cost of a growing static response. Thanks to the closed-form character of the tuning method, this problem can be tackled and minimized. However, due to this static softening, the here proposed tuning rules might not be suitable for every application.

Furthermore, the two approaches have been compared more thoroughly in terms of their stability margins and implementation by using the open-loop transfer functions of the controlled systems. While we can draw an analogy between the two approaches for their tuning parameters and their receptance functions, their stability margins differ. This can be attributed to the different implementation of what is considered a plant and what is considered a feedback. The optimal NC shunt exhibits an extremely small phase margin, disqualifying it for a practical implementation. The NC should therefore be chosen according to a trade-off between performance improvement and robustness margins. By contrast, the optimal PPF controller exhibits better stability margins, which makes it viable in a practical application.

This work builds the basis for a new PPF controller tuning to mitigate structural vibrations. Future works will include a study about the positions of the sensor-actuator pair and a practical implementation of the method for the demonstration of the here derived tuning rule.

Acknowledgements

The authors J. Dietrich, G. Raze and G. Kerschen would like to acknowledge the financial support of the SPW (WALInnov grant 1610122).

References

[1] N. W. Hagood and A. von Flotow, "Damping of structural vibrations with piezoelectric materials and passive electrical networks," *Journal of Sound and Vibration*, vol. 146, no. 2, 1991.

[2] T. Asami and O. Nishihara, "Closed-Form Exact Solution to H_∞ Optimization of Dynamic Vibration Absorbers (Application to Different Transfer Functions and Damping Systems)," *Journal of Vibration and Acoustics*, vol. 125, pp. 398–405, Jul. 2003.

[3] P. Soltani, G. Kerschen, G. Tondreau, and A. Deraemaeker, "Piezoelectric vibration damping using resonant shunt circuits: an exact solution," *Smart Materials and Structures*, vol. 23, no. 12, 2014.

[4] M. Neubauer, R. Oleskiewicz, K. Popp, and T. Krzyzynski, "Optimization of damping and absorbing performance of shunted piezo elements utilizing negative capacitance," *Journal of Sound and Vibration*, vol. 298, pp. 84–107, Nov. 2006.

[5] G. Raze, A. Jadoul, S. Guichaux, V. Broun, and G. Kerschen, "A digital nonlinear piezoelectric tuned vibration absorber," *Smart Materials and Structures*, vol. 29, no. 1, Jan. 2020.

[6] R. L. Forward, "Electromechanical transducer-coupled mechanical structure with negative capacitance compensation circuit," U.S. Patent 4 158 787, Jun., 1979.

[7] D. Bondoux, "Piezodamping: a low-power-consumption technique for semi-active damping of light structures," Lyon, France, Apr. 1996, p. 694.

[8] J. Tang and K. W. Wang, "Active-passive hybrid piezoelectric networks for vibration control: comparisons and improvement," *Smart Mater. Struct.*, vol. 10, no. (2001) 794–806, Jul. 2001.

[9] S. Behrens, A. J. Fleming, and S. O. R. Moheimani, "A broadband controller for shunt piezoelectric damping of structural vibration," *Smart Materials and Structures*, vol. 12, no. 1, jan 2003.

[10] B. de Marneffe and A. Preumont, "Vibration damping with negative capacitance shunts: theory and experiment," *Smart Materials and Structures*, vol. 17, no. 3, p. 035015, Jun. 2008.

[11] M. Berardengo, O. Thomas, C. Giraud-Audine, and S. Manzoni, "Improved resistive shunt by means of negative capacitance: new circuit, performances and multi-mode control," *Smart Materials and Structures*, vol. 25, no. 7, Jul. 2016.

[12] M. Berardengo, S. Manzoni, O. Thomas, and M. Vanali, "Piezoelectric resonant shunt enhancement by negative capacitances: Optimisation, performance and resonance cancellation," *Journal of Intelligent Material Systems and Structures*, vol. 29, no. 12, pp. 2581–2606, Jul. 2018.

[13] M. Berardengo, S. Manzoni, M. Vanali, and R. Bonsignori, "Enhancement of the broadband vibration attenuation of a resistive piezoelectric shunt," *Journal of Intelligent Material Systems and Structures*, Jan. 2021.

[14] J. L. Fanson and T. K. Caughey, "Positive position feedback control for large space structures," *AIAA Journal*, vol. 28, no. 4, Apr. 1990.

[15] A. Paknejad, G. Zhao, M. Osée, A. Deraemaeker, F. Robert, and C. Collette, "A novel design of positive position feedback controller based on maximum damping and H_2 optimization," *Journal of Vibration and Control*, vol. 26, no. 15-16, Aug. 2020.

[16] G. Zhao, A. Paknejad, G. Raze, A. Deraemaeker, G. Kerschen, and C. Collette, "Nonlinear positive position feedback control for mitigation of nonlinear vibrations," *Mechanical Systems and Signal Processing*, vol. 132, pp. 457–470, Oct. 2019.

[17] G. S. Agnes, "Performance of Nonlinear Mechanical, Resonant-Shunted Piezoelectric, and Electronic Vibration Absorbers for Multi-Degree-of-Freedom Structures," Doctoral Thesis, Virginia State University, 1997.

[18] J. F. Toftekær, A. Benjeddou, and J. Høgsberg, "General numerical implementation of a new piezoelectric shunt tuning method based on the effective electromechanical coupling coefficient," *Mechanics of Advanced Materials and Structures*, vol. 27, no. 22, pp. 1908–1922, Nov. 2020.

[19] T. Ikegame, K. Takagi, and T. Inoue, "Exact Solutions to H_∞ and H_2 Optimizations of Passive Resonant Shunt Circuit for Electromagnetic or Piezoelectric Shunt Damper," *Journal of Vibration and Acoustics*, vol. 141, Jun. 2019.

[20] W. R. Inc., "Mathematica, Version 12.2," champaign, IL, 2020. [Online]. Available: https://www.wolfram.com/wolfram-alpha-notebook-edition

[21] G. Zhao, A. Paknejad, G. Raze, G. Kerschen, and C. Collette, "H_∞ optimization of positive position feedback control for mitigation of nonlinear vibrations," in *Conference Proceedings of ISMA2018 - USD2018*, Leuven, Sep. 2018.

[22] G. F. Franklin, J. D. Powell, and M. L. Workman, *Digital control of dynamic systems*, 2nd ed. Reading, Mass: Addison-Wesley, 1990.

[23] G. Raze, J. Dietrich, and G. Kerschen, "Onset and stabilization of delay-induced instabilities in piezoelectric digital vibration absorbers," *Journal of Intelligent Material Systems and Structures*, p. 1045389X2110722, Jan. 2022.